Elastic and sound orthonormal beams and localized fields in linear media: III. Superpositions of transverse elastic plane waves in an isotropic medium

2001 J. Phys. A: Math. Gen. 34 6269

(http://iopscience.iop.org/0305-4470/34/32/306)

INSTITUTE OF PHYSICS PUBLISHING JOURNAL OF PHYSICS A: MATHEMATICAL AND GENERAL

J. Phys. A: Math. Gen. **34** (2001) 6269–6279 PII: S0305-4470(01)19770-2

Elastic and sound orthonormal beams and localized fields in linear media: III. Superpositions of transverse elastic plane waves in an isotropic medium

George N Borzdov

Department of Theoretical Physics, Belarusian State University, Fr. Skaryny avenue 4, 220050 Minsk, Belarus

Received 29 November 2000, in final form 13 June 2001
Published 3 August 2001
Online at stacks.iop.org/JPhysA/34/6269

Abstract

Unique families of time-harmonic orthonormal beams and localized fields in an isotropic linear elastic medium are presented. They are obtained using expansions in transverse plane waves whose intensities and phases are specified by the spherical harmonics. The families of orthonormal beams can be used as functional bases for complex elastic fields. As in the case of fields formed from longitudinal plane waves, the presented localized fields include elastic storms, whirls and tornadoes. The orthonormal beams and the localized fields are illustrated by calculating fields, energy densities and energy fluxes.

PACS numbers: 62.30.+d, 43.20.+g, 02.30.Nw

1. Introduction

To compose a field from harmonic plane waves (eigenwaves) in a linear medium, one must specify propagation directions, frequencies or wavenumbers, polarizations, intensities and phases of all eigenwaves forming the field. It is advantageous [1–5] to set the intensities and the phases by a set of orthonormal scalar functions on a two- or three-dimensional manifold. This approach was originally developed for electromagnetic [1–3] and weak gravitational [3] fields. In the first paper [4] of this series, we extended it to elastic fields in isotropic and anisotropic media and sound waves in an ideal liquid. In the second paper [5], we applied it to fields in an isotropic elastic medium, composed from longitudinal eigenwaves as

$$\boldsymbol{W}_j^s(\boldsymbol{r}, t) = \exp(-\mathrm{i}\omega t) \int_0^{2\pi} \mathrm{d}\varphi \int_0^{\theta_2} \exp[\mathrm{i}\boldsymbol{r} \cdot \boldsymbol{k}(\theta, \varphi)] Y_j^s(\theta, \varphi) \nu(\theta, \varphi) \boldsymbol{W}(\theta, \varphi) \sin\theta \, \mathrm{d}\theta \qquad (1)$$

where $\boldsymbol{W} = \boldsymbol{W}(\theta, \varphi)$ and $\nu = \nu(\theta, \varphi)$ are the amplitude and the beam state functions [4, 5]. Intensities and phases of these eigenwaves are defined by the spherical harmonics Y_j^s, and propagation directions are given by

$$\hat{\boldsymbol{k}} = \boldsymbol{k}/k = \boldsymbol{e}_\mathrm{r} = \sin\theta'(\boldsymbol{e}_1 \cos\varphi + \boldsymbol{e}_2 \sin\varphi) + \boldsymbol{e}_3 \cos\theta' \qquad (2)$$

where $\boldsymbol{e}_{\mathrm{r}}$ is the radial basis vector of the spherical coordinate system, $(\boldsymbol{e}_{\mathrm{i}})$ are the Cartesian basis vectors, $\theta' = \kappa_0\theta$ and parameter κ_0 satisfies the condition $0 < \kappa_0 \leqslant 1$. These fields are formed from plane waves propagating in the solid angle $\Omega = 2\pi(1 - \cos\kappa_0\theta_2)$.

In this paper, we consider elastic fields formed from transverse eigenwaves propagating in an isotropic medium. Although they are described by the above equations as well, the amplitude function $\boldsymbol{W} = \boldsymbol{W}(\theta, \varphi)$ is now of a completely different type. A transverse elastic eigenwave has the two-dimensional amplitude subspace, and its displacement vector $\boldsymbol{u}$ satisfies the condition $\boldsymbol{u} \cdot \hat{\boldsymbol{k}} = 0$. In accordance with the general relations presented in [4], we set two amplitude functions as follows:

$$\boldsymbol{W}(\theta, \varphi) \equiv \begin{pmatrix} \boldsymbol{u} \\ \boldsymbol{f} \end{pmatrix} = \begin{pmatrix} \boldsymbol{e}_{\theta'} \\ \mathrm{i}k\mu_{\mathrm{L}}\left(-\sin\theta'\boldsymbol{e}_{\mathrm{r}} + \cos\theta'\boldsymbol{e}_{\theta'}\right) \end{pmatrix} \tag{3}$$

$$\boldsymbol{W}(\theta, \varphi) \equiv \begin{pmatrix} \boldsymbol{u} \\ \boldsymbol{f} \end{pmatrix} = \begin{pmatrix} \boldsymbol{e}_{\varphi} \\ \mathrm{i}k\mu_{\mathrm{L}}\cos\theta'\boldsymbol{e}_{\varphi} \end{pmatrix} \tag{4}$$

where

$$\boldsymbol{e}_{\theta'} = \cos\theta'(\boldsymbol{e}_1\cos\varphi + \boldsymbol{e}_2\sin\varphi) - \boldsymbol{e}_3\sin\theta' \tag{5}$$

$$\boldsymbol{e}_{\varphi} = -\boldsymbol{e}_1\sin\varphi + \boldsymbol{e}_2\cos\varphi \tag{6}$$

are the spherical basis vectors, $\boldsymbol{f} = \sigma\boldsymbol{e}_3$ is the force density, σ is the stress tensor, $k = 2\pi/\lambda = \omega/v_2$ is the wavenumber, $v_2 = \sqrt{\mu_{\mathrm{L}}/\varrho}$ is the phase velocity, μ_{L} is the Lamé module [6] and ϱ is the medium density. This gives two different families of beams (u_{M}-beams or u_{A}-beams), composed from eigenwaves with the meridional and azimuthal orientation of $\boldsymbol{u}$, respectively. In this series of papers, we separately treat elastic beams composed of longitudinal and transverse eigenwaves, as well as u_{M} and u_{A}-beams. Plane wave superpositions including different types of elastic wave, e.g., longitudinal and transverse, can be conveniently described by making use of the exponential evolution operators [7].

The outline of the paper is as follows. Families of elastic orthonormal beams and localized fields are presented in sections 2 and 3, respectively. The results are summarized in section 4.

2. Orthonormal beams

2.1. Orthonormal beams with $\theta_2 = \pi/2$, $\kappa_0 = 1$ and $\Omega = 2\pi$

Let us first consider the family of orthonormal beams $\boldsymbol{W}_j^s$ (1) with $\theta_2 = \pi/2$ and $\kappa_0 = 1$ ($\theta' = \theta$), which are formed from eigenwaves propagating into a solid angle $\Omega = 2\pi$. As for the similar beams formed from longitudinal eigenwaves [5], the orthonormalizing function [4] $\nu = \nu(\theta, \varphi)$ reduces to a constant upon substitution of both amplitude functions $\boldsymbol{W}$ (3) and $\boldsymbol{W}$ (4). As a consequence, we obtain the $\boldsymbol{u}_{\mathrm{M}}$-beam,

$$\boldsymbol{u} = \nu_2 \mathrm{e}^{\mathrm{i}(s\psi - \omega t)}\boldsymbol{u}_0 \tag{7}$$

$$\boldsymbol{f} = \mathrm{i}k\mu_{\mathrm{L}}\nu_2\mathrm{e}^{\mathrm{i}(s\psi-\omega t)}\left\{\boldsymbol{e}I_j^{ss-1}[\cos\circ 2] + \boldsymbol{e}^*I_j^{ss+1}[\cos\circ 2] - \boldsymbol{e}_3 I_j^{ss}[\sin\circ 2]\right\}, \tag{8}$$

and the $\boldsymbol{u}_{\mathrm{A}}$-beam,

$$\boldsymbol{u} = \mathrm{i}\nu_2\mathrm{e}^{\mathrm{i}(s\psi-\omega t)}\left(\boldsymbol{e}^*I_j^{ss+1}[1] - \boldsymbol{e}I_j^{ss-1}[1]\right) \tag{9}$$

$$\boldsymbol{f} = k\mu_{\mathrm{L}}\nu_2\mathrm{e}^{\mathrm{i}(s\psi-\omega t)}\left(\boldsymbol{e}I_j^{ss-1}[\cos] - \boldsymbol{e}^*I_j^{ss+1}[\cos]\right), \tag{10}$$

where

$$\boldsymbol{u}_0 = \boldsymbol{e}I_j^{ss-1}[\cos] + \boldsymbol{e}^*I_j^{ss+1}[\cos] - \boldsymbol{e}_3 I_j^{ss}[\sin] \tag{11}$$

$$\nu_2 = \frac{1}{\pi}\sqrt{\frac{N_Q}{\varrho v_2^3}} \qquad \boldsymbol{e} = (\boldsymbol{e}_{\mathrm{R}} + \mathrm{i}\boldsymbol{e}_{\mathrm{A}})/2 \tag{12}$$

$$\boldsymbol{e}_{\mathrm{R}} = \boldsymbol{e}_1 \cos\psi + \boldsymbol{e}_2 \sin\psi \qquad \boldsymbol{e}_{\mathrm{A}} = -\boldsymbol{e}_1 \sin\psi + \boldsymbol{e}_2 \cos\psi \tag{13}$$

$$\boldsymbol{r} = R\boldsymbol{e}_{\mathrm{R}} + z\boldsymbol{e}_3 \qquad R = r\sin\gamma \qquad z = r\cos\gamma. \tag{14}$$

Here, N_Q is the normalizing constant [4], R, ψ and z are the cylindrical coordinates of the point with radius vector $\boldsymbol{r}$ and r, γ and ψ are the spherical coordinates of the same point. The real and imaginary parts of complex scalar function $I_j^{sm}[f] = I_j^{sm}[f](r,\gamma)$ can be separated as [2,4]

$$I_j^{sm}[f] = \mathrm{i}^{|m|}(J_{j0}^{sm}[f] + \mathrm{i}J_{j1}^{sm}[f]). \tag{15}$$

Both functions $I_j^{sm}[f]$ and $J_{jp}^{sm}[f]$ $(p = 0, 1)$ are defined by the spherical harmonic $Y_j^s = Y_j^s(\theta,\varphi)$, an integer m and a scalar function $f = f(\theta)$. For any given f, they are functions of r and γ. At fixed r and γ, they are functionals regarding f. The definitions and the properties of these functions are presented in [2,4]. When it cannot cause a misunderstanding, we omit the arguments (r,γ).

The deformation γ and stress σ tensor fields of the $\boldsymbol{u}_{\mathrm{M}}$-beam (7) have the form

$$\gamma = \frac{\sigma}{2\mu_{\mathrm{L}}} = \mathrm{i}k\nu_2 \mathrm{e}^{\mathrm{i}(s\psi-\omega t)}\gamma_0 \tag{16}$$

where

$$\gamma_0 = \tfrac{1}{2}\rho I_j^{ss-2}[\sin\circ 2] + \tfrac{1}{2}\rho^* I_j^{ss+2}[\sin\circ 2] + \rho_2 I_j^{ss-1}[\cos\circ 2] + \rho_2^* I_j^{ss+1}[\cos\circ 2]$$
$$+\tfrac{1}{2}\left(\rho_1 - \rho_3\right) I_j^{ss}[\sin\circ 2] \tag{17}$$

$$\rho = \boldsymbol{e}\otimes\boldsymbol{e} \qquad \rho_1 = \boldsymbol{e}\otimes\boldsymbol{e}^* + \boldsymbol{e}^*\otimes\boldsymbol{e} = \tfrac{1}{2}(\mathbf{1} - \rho_3) \tag{18}$$

$$\rho_2 = \tfrac{1}{2}(\boldsymbol{e}\otimes\boldsymbol{e}_3 + \boldsymbol{e}_3\otimes\boldsymbol{e}) \qquad \rho_3 = \boldsymbol{e}_3\otimes\boldsymbol{e}_3 \tag{19}$$

and $\mathbf{1}$ is the unit dyadic.

Using the expressions $\boldsymbol{u}$ (7), γ and σ (16), we also obtain the kinetic w_{K} and the elastic w_{E} energy densities, the energy flux density vector $\boldsymbol{S}$ (see [4,6] for the definitions of these quantities) and the normal component S_3 of $\boldsymbol{S}$ as follows:

$$w_{\mathrm{K}} = w_0 w_{\mathrm{M}} \qquad w_0 = S_0/v_2 \qquad S_0 = N_Q/\lambda^2 \tag{20}$$

$$w_{\mathrm{M}} = \sum_{p=0}^{1}\left\{\tfrac{1}{2}\left(J_{jp}^{ss-1}[\cos]\right)^2 + \tfrac{1}{2}\left(J_{jp}^{ss+1}[\cos]\right)^2 + \left(J_{jp}^{ss}[\sin]\right)^2\right\} \tag{21}$$

$$w_{\mathrm{E}} = \frac{w_0}{2}\sum_{p=0}^{1}\left\{\frac{1}{4}(J_{jp}^{ss-2}[\sin\circ 2])^2 + \frac{1}{4}(J_{jp}^{ss+2}[\sin\circ 2])^2 + (J_{jp}^{ss-1}[\cos\circ 2])^2\right.$$
$$\left.+(J_{jp}^{ss+1}[\cos\circ 2])^2 + \frac{3}{2}(J_{jp}^{ss}[\sin\circ 2])^2\right\} \tag{22}$$

$$\boldsymbol{S} = S_0\boldsymbol{S}' = 4S_0\Re\left(\gamma_0\boldsymbol{u}_0^*\right) \tag{23}$$

$$S_{\mathrm{N}}' = \frac{S_3}{S_0} = \sum_{p=0}^{1}\left\{J_{jp}^{ss-1}[\cos]J_{jp}^{ss-1}[\cos\circ 2] + J_{jp}^{ss+1}[\cos]J_{jp}^{ss+1}[\cos\circ 2]\right.$$
$$\left.+2J_{jp}^{ss}[\sin]J_{jp}^{ss}[\sin\circ 2]\right\}. \tag{24}$$

Similarly, for the u_{A}-beam (9), we obtain

$$\gamma = \frac{\sigma}{2\mu_{\mathrm{L}}} = k\nu_2\mathrm{e}^{\mathrm{i}(s\psi-\omega t)}\left\{\rho I_j^{ss-2}[\sin] - \rho^* I_j^{ss+2}[\sin] + \rho_2 I_j^{ss-1}[\cos] - \rho_2^* I_j^{ss+1}[\cos]\right\} \tag{25}$$

$$w_{\mathrm{K}} = w_0 w_{\mathrm{A}} \qquad w_{\mathrm{A}} = \frac{1}{2}\sum_{p=0}^{1}\left\{\left(J_{jp}^{ss-1}[1]\right)^2 + \left(J_{jp}^{ss+1}[1]\right)^2\right\} \tag{26}$$

$$w_{\mathrm{E}} = \frac{w_0}{2}\sum_{p=0}^{1}\left\{(J_{jp}^{ss-2}[\sin])^2 + (J_{jp}^{ss+2}[\sin])^2 + (J_{jp}^{ss-1}[\cos])^2 + (J_{jp}^{ss+1}[\cos])^2\right\} \tag{27}$$

$$\boldsymbol{S} = S_0(S'_{\mathrm{R}}\boldsymbol{e}_{\mathrm{R}} + S'_{\mathrm{A}}\boldsymbol{e}_{\mathrm{A}} + S'_{\mathrm{N}}\boldsymbol{e}_3) \tag{28}$$

where

$$S'_{\mathrm{R}} = \sum_{p=0}^{1}(-1)^p\left\{\beta(1-s)J_{jp}^{ss-2}[\sin]J_{j1-p}^{ss-1}[1] + \beta(s+1)J_{jp}^{ss+2}[\sin]J_{j1-p}^{ss+1}[1]\right\} \tag{29}$$

$$S'_{\mathrm{A}} = \sum_{p=0}^{1}\left\{\beta(s+1)J_{jp}^{ss+2}[\sin]J_{jp}^{ss+1}[1] - \beta(1-s)J_{jp}^{ss-2}[\sin]J_{jp}^{ss-1}[1]\right\} \tag{30}$$

$$S'_{\mathrm{N}} = \sum_{p=0}^{1}\left\{J_{jp}^{ss-1}[\cos]J_{jp}^{ss-1}[1] + J_{jp}^{ss+1}[\cos]J_{jp}^{ss+1}[1]\right\} \tag{31}$$

$$\beta(s) = \begin{cases} -1 & (s = -1, -2, \ldots) \\ 1 & (s = 0, 1, 2, \ldots). \end{cases} \tag{32}$$

The energy fluxes and the energy densities of u_{M} and u_{A} beams are illustrated in figures 1 and 2. These elastic beams bear some similarities to the electromagnetic beams treated in [1–3]. In particular, the displacement fields for both $\boldsymbol{u}_{\mathrm{M}}$ beams (7) and $\boldsymbol{u}_{\mathrm{A}}$ beams (9) are described by the same functions as for the corresponding electric or magnetic field in [2]. As a result, the kinetic energy densities w_{K} (20), w_{K} (26) and the energy densities w_{e} and w_{m} of electric and magnetic fields are also specified by the same functions w_{M} (21) and w_{A} (26), so figures 1 and 2 in [2] illustrate the properties of both electromagnetic and elastic beams. The u_{A}-beam bears an even closer resemblance. It is described by the same normal component S'_{N} (31) of the normalized energy flux density vector $\boldsymbol{S}'$ as the corresponding electromagnetic beam (see figure 4 in [2]).

The distinction between elastic and electromagnetic beams manifests itself in the second component ($\boldsymbol{f}$ for elastic beams and $\boldsymbol{E}$ or $\boldsymbol{H}$ vector for electromagnetic beams) of the block vector $\boldsymbol{W}$ which enters into the orthogonality condition [2, 4]. The coordinate dependence of $\boldsymbol{f}$ (8) and $\boldsymbol{f}$ (10) differs from the coordinate dependence of $\boldsymbol{E}$ and $\boldsymbol{H}$. For the transverse and longitudinal elastic beams, $\boldsymbol{f}$ can be calculated from the corresponding stress tensor $\boldsymbol{f} = \sigma\boldsymbol{e}_3$.

Figure 2 illustrates similarities of and distinctions between the energy distributions of u_{M}- and u_{A}-beams defined by the same spherical harmonic Y_3^1. Both beams are highly localized in all directions, and for them w' reaches its maximum values in the planes $z' = \pm 0.7$ instead of the symmetry plane $z = 0$. However, for the u_{A}-beam these maxima are reached exactly at the z-axis, whereas for the u_{M}-beams they are reached at distance $R' = 0.3$ from this axis. Besides, the peak of w' for the u_{A}-beam is twice as large as that of the u_{M} beam.

Of the two types of transverse elastic beam, the azimuthal beams are simpler in structure. In particular, for the u_{A}-beam defined by the zonal spherical harmonic Y_j^0, from equations (9), (10) and (25)–(31), we obtain

$$\boldsymbol{u} = \boldsymbol{e}_{\mathrm{A}}\nu_2 \mathrm{e}^{-\mathrm{i}\omega t} I_j^{01}[1] \qquad \boldsymbol{f} = \mathrm{i}\boldsymbol{e}_{\mathrm{A}} k\mu_{\mathrm{L}}\nu_2 \mathrm{e}^{-\mathrm{i}\omega t} I_j^{01}[\cos] \tag{33}$$

$$\sigma = 2\mu_{\mathrm{L}}\gamma = \mathrm{i}k\mu_{\mathrm{L}}\nu_2 \mathrm{e}^{-\mathrm{i}\omega t}\left\{\left(\boldsymbol{e}_{\mathrm{A}}\otimes\boldsymbol{e}_3 + \boldsymbol{e}_3\otimes\boldsymbol{e}_{\mathrm{A}}\right)I_j^{01}[\cos] + \left(\boldsymbol{e}_{\mathrm{R}}\otimes\boldsymbol{e}_{\mathrm{A}} + \boldsymbol{e}_{\mathrm{A}}\otimes\boldsymbol{e}_{\mathrm{R}}\right)I_j^{02}[\sin]\right\} \tag{34}$$

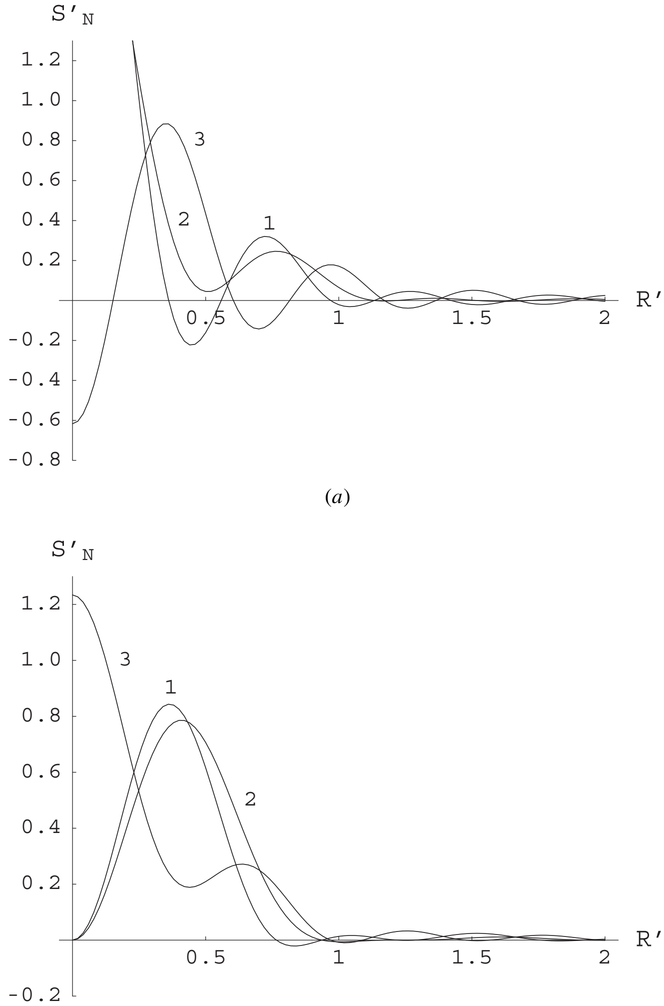

Figure 1. Normal component $S'_{\rm N}$ of the normalized energy flux vector of (*a*) $u_{\rm M}$ and (*b*) $u_{\rm A}$ elastic beams as a function of $R' = R/\lambda$; $z = 0$; $\lambda_{\rm L}/\mu_{\rm L} = 7/9$; $\theta_2 = \pi/2$; $\kappa_0 = 1$; $\Omega = 2\pi$; $j = s = 0$ (curve 1; $S'_{\rm N}(0) = 3.29$ for $u_{\rm M}$-beam); $j = 1$, $s = 0$ (curve 2; $S'_{\rm N}(0) = 2.468$ for $u_{\rm M}$-beam); $j = s = 1$ (curve 3).

$$w_{\rm K} = w_0 \sum_{p=0}^{1} \left(J_{jp}^{01}[1]\right)^2 \qquad w_{\rm E} = w_0 \sum_{p=0}^{1} \left\{\left(J_{jp}^{01}[\cos]\right)^2 + \left(J_{jp}^{02}[\sin]\right)^2\right\} \tag{35}$$

$$S'_{\rm R} = 2 \sum_{p=0}^{1} (-1)^p J_{jp}^{02}[\sin] J_{j1-p}^{01}[1] \qquad S'_{\rm N} = 2 \sum_{p=0}^{1} J_{jp}^{01}[\cos] J_{jp}^{01}[1]. \tag{36}$$

The azimuthal component $S_{\rm A}$ of the time-average energy flux density vector $\boldsymbol{S}$ is zero at all points.

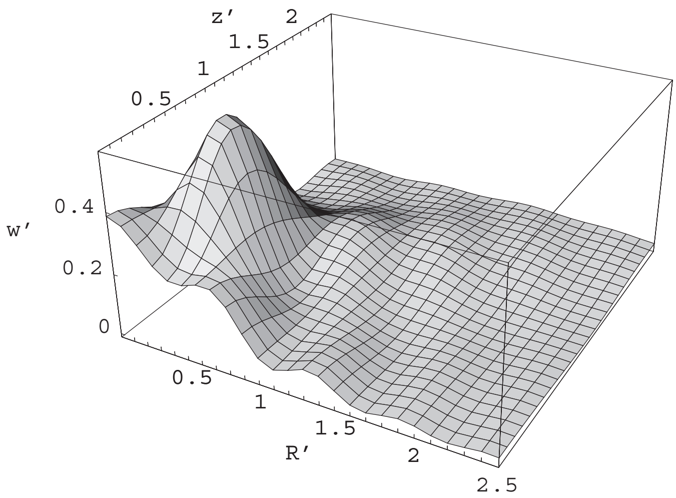

(*a*)

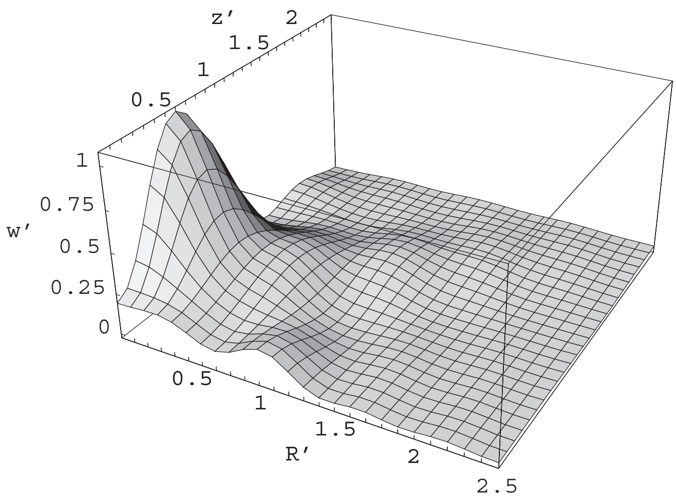

(*b*)

Figure 2. Normalized energy density $w' = (w_K + w_E)/w_0$ of (*a*) u_M and (*b*) u_A elastic beams as a function of cylindrical coordinates $R' = R/\lambda$ and $z' = z/\lambda$; $\lambda_L/\mu_L = 7/9$; $\theta_2 = \pi/2$; $\kappa_0 = 1$; $\Omega = 2\pi$; $j = 3$; $s = 1$.

2.2. Orthonormal beams with $\theta_2 = \pi$, $\kappa_0 \leqslant 1/2$ and $\Omega \leqslant 2\pi$

For the fields treated above, the beam manifold $\mathcal{B}$ [4] is the northern hemisphere S^2_N of the unit sphere S^2, whereas the spherical harmonics (Y^s_j) comprise a complete orthonormal system on the entire sphere S^2. This is why these fields can be grouped into two separate sets of orthonormal beams, defined by the spherical harmonics Y^s_j with even and odd j, respectively.

To obtain a complete system of orthonormal beams [2, 4], defined by the whole set of spherical harmonics, we set $\theta_2 = \pi$ and $\kappa_0 \leqslant 1/2$. In this case, eigenwaves forming the beams propagate in the solid angle $\Omega = 2\pi(1 - \cos\kappa_0\pi) \leqslant 2\pi$, and the beam manifold is the unit

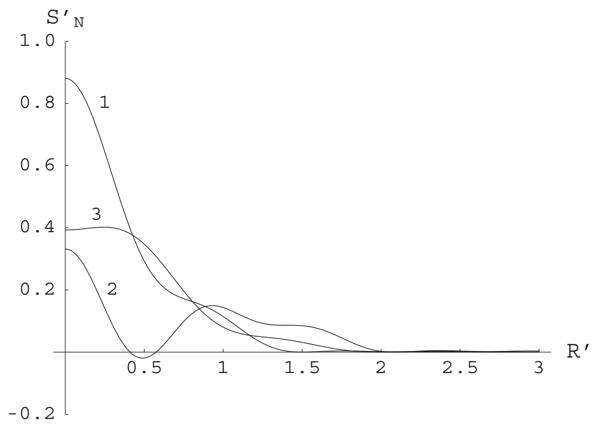

(*a*)

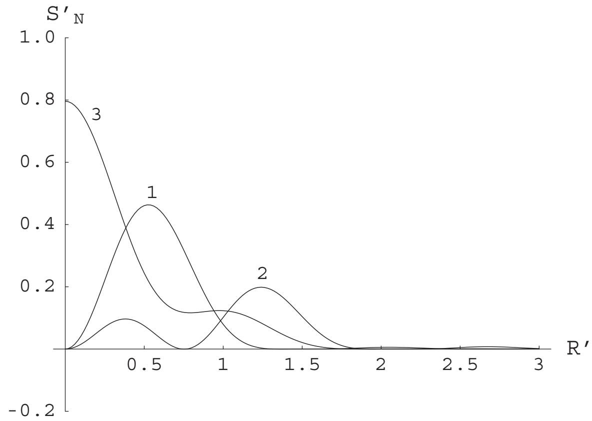

(*b*)

Figure 3. Normal component $S'_{\rm N}$ of the normalized energy flux vector of (*a*) $u_{\rm M}$ and (*b*) $u_{\rm A}$ elastic beams as a function of $R' = R/\lambda$; $z = 0$; $\lambda_{\rm L}/\mu_{\rm L} = 7/9$; $\theta_2 = \pi$; $\kappa_0 = 0.3$; $\Omega = 2\pi[1 - \cos(0.3\pi)]$; $j = s = 0$ (curve 1); $j = 1$, $s = 0$ (curve 2); $j = s = 1$ (curve 3).

sphere ($\mathcal{B} = S^2$). For both $\boldsymbol{u}_{\rm M}$- and $\boldsymbol{u}_{\rm A}$-beams, the orthonormalizing function [4] becomes

$$\nu(\theta) = \frac{1}{\pi}\sqrt{\frac{\kappa_0 N_Q \sin\kappa_0\theta}{2\varrho v_2^3 \sin\theta}}. \qquad (37)$$

Parameter κ_0 exerts primary control over the beam divergence and the dimensions of the beam cross-section at the plane $z = 0$. The smaller κ_0, the more collimated is the beam, but the cross-section becomes larger (compare figures 1 and 3). Conversely, beams with $\kappa_0 = 1/2$ and $\Omega = 2\pi$ have a pronounced core region. When $s \neq 0$ and $\kappa_0 = 1/2$ or $\kappa_0 \approx 1/2$, such beams have spiral energy fluxes and resemble elastic tornadoes.

3. Localized fields

In the previous paper [5], we presented three unique families of localized elastic fields formed from longitudinal waves propagating in an isotropic medium: elastic storms, whirls and

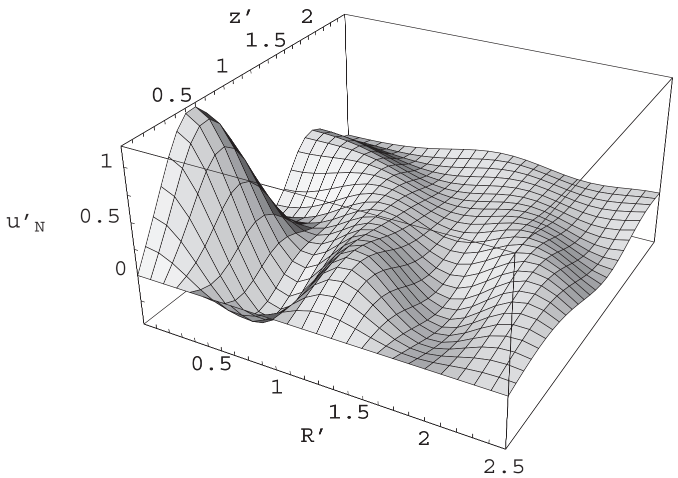

(*a*)

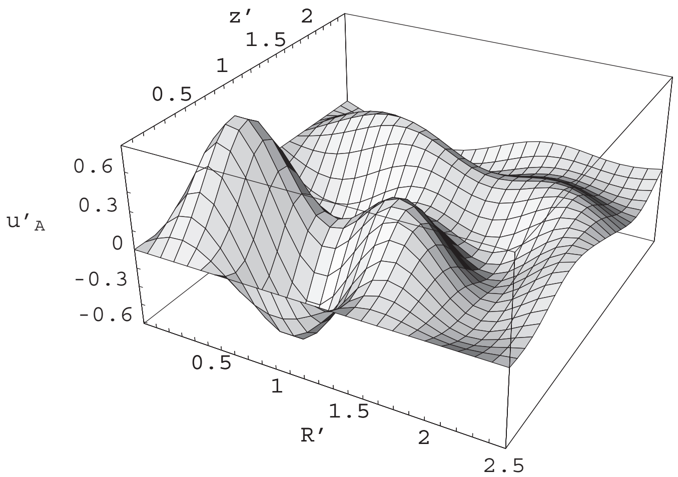

(*b*)

Figure 4. (*a*) Normal u'_{N} and (*b*) azimuthal u'_{A} components of the normalized instantaneous displacement field $\boldsymbol{u}' = (\Re\, \boldsymbol{u})/u_n$ ($u_n = (2/\omega)\sqrt{w_0/\rho}$) of (*a*) u_{M} and (*b*) u_{A} elastic storms as functions of $R' = R/\lambda$ and $z' = z/\lambda$; $\lambda_{\mathrm{L}}/\mu_{\mathrm{L}} = 7/9$; $\theta_2 = \pi$; $\kappa_0 = 1$; $\Omega = 4\pi$; $j = 3$; $s = 0$; (*a*) $\omega t = \pi/4$; (*b*) $t = 0$.

tornadoes. In this section, we present similar elastic fields formed from transverse eigenwaves. They are described by equation (1) with $\pi/2 \leqslant \theta_2 \leqslant \pi$ and $\kappa_0 = 1$ ($\theta' = \theta$). We assume that the beam state function $\nu = \nu(\theta, \varphi)$ reduces to a constant.

3.1. Storms and whirls

When $\theta_2 = \pi$, equation (1) describes three-dimensional standing waves composed from eigenwaves of all possible propagation directions ($\mathcal{B} = S^2$ and $\Omega = 4\pi$). There are two basically different types of such fields—storms (see figure 4) and whirls (see figure 5)—which are defined by Y_j^s with $s = 0$ and $s \neq 0$, respectively.

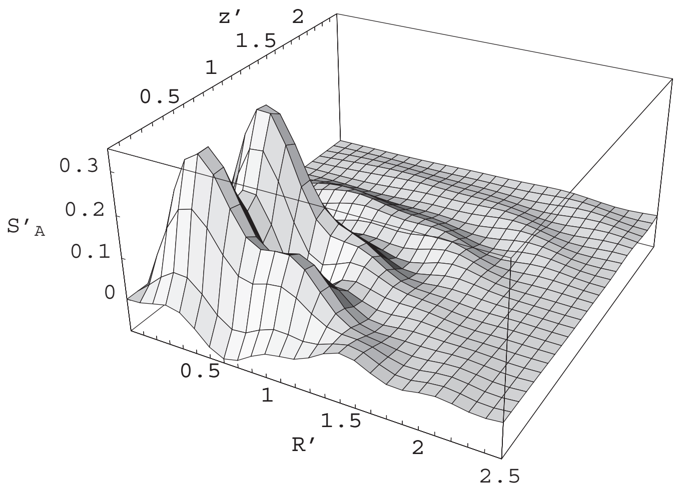

(*a*)

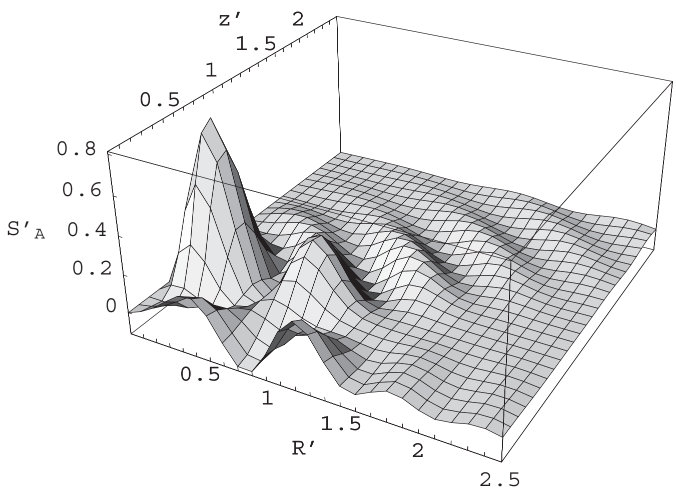

(*b*)

Figure 5. Azimuthal component S'_{A} of the normalized energy flux vector of (*a*) u_{M} and (*b*) u_{A} elastic whirls as a function of $R' = R/\lambda$ and $z' = z/\lambda$; $\lambda_{\mathrm{L}}/\mu_{\mathrm{L}} = 7/9$; $\theta_2 = \pi$; $\kappa_0 = 1$; $\Omega = 4\pi$; $j = 4$; $s = 2$.

Substitution of $\boldsymbol{W}$ (3) and $\boldsymbol{W}$ (4) into equation (1) with $\theta_2 = \pi$ results in two types of standing wave composed of transverse elastic waves, namely, the u_{M}-wave

$$u = \sqrt{2}\nu_2 \mathrm{e}^{\mathrm{i}(s\psi-\omega t)}\left\{\boldsymbol{e}\,\mathrm{i}^{|s-1|+q} J_{jq}^{ss-1}[\cos] + \boldsymbol{e}^*\mathrm{i}^{|s+1|+q} J_{jq}^{ss+1}[\cos] - \boldsymbol{e}_3 \mathrm{i}^{|s|+p} J_{jp}^{ss}[\sin]\right\} \tag{38}$$

$$\boldsymbol{f} = \mathrm{i}^{|s|+q+1}\sqrt{2}k\nu_2\mu_{\mathrm{L}}\mathrm{e}^{\mathrm{i}(s\psi-\omega t)}\left\{\boldsymbol{e}(-1)^p\beta(-s)J_{jp}^{ss-1}[\cos\circ 2] + \boldsymbol{e}^*(-1)^p\beta(s)J_{jp}^{ss+1}[\cos\circ 2] - \boldsymbol{e}_3 J_{jq}^{ss}[\sin\circ 2]\right\} \tag{39}$$

and the u_{A}-wave

$$\boldsymbol{u} = \mathrm{i}\sqrt{2}\nu_2\mathrm{e}^{\mathrm{i}(s\psi-\omega t)}\left\{\boldsymbol{e}^*\mathrm{i}^{|s+1|+p}J_{jp}^{ss+1}[1] - \boldsymbol{e}\,\mathrm{i}^{|s-1|+p}J_{jp}^{ss-1}[1]\right\} \tag{40}$$

$$\boldsymbol{f} = \sqrt{2}k\nu_2\mu_{\mathrm{L}}\mathrm{e}^{\mathrm{i}(s\psi-\omega t)}\left\{\boldsymbol{e}\,\mathrm{i}^{|s-1|+q}J_{jq}^{ss-1}[\cos] - \boldsymbol{e}^*\mathrm{i}^{|s+1|+q}J_{jq}^{ss+1}[\cos]\right\}. \tag{41}$$

Here, $p = 1 - q = 0$ if $j + |s|$ is even, and $p = 1 - q = 1$ if $j + |s|$ is odd.

The stress σ and deformation γ tensor fields are described by

$$\begin{aligned}\sigma = 2\mu_L\gamma = {} & \mathrm{i}^{|s|+q+1}\sqrt{2}k\nu_2\mu_L e^{\mathrm{i}(s\psi-\omega t)}\big\{\rho\alpha(s)J_{jq}^{ss-2}[\sin\circ 2] + \rho^*\alpha(-s)J_{jq}^{ss+2}[\sin\circ 2]\\ & +2\rho_2(-1)^p\beta(-s)J_{jp}^{ss-1}[\cos\circ 2] + 2\rho_2^*(-1)^p\beta(s)J_{jp}^{ss+1}[\cos\circ 2]\\ & +(\rho_1-\rho_3)J_{jq}^{ss}[\sin\circ 2]\big\}\end{aligned} \qquad (42)$$

for the u_M-wave, and

$$\begin{aligned}\sigma = 2\mu_L\gamma = {} & 2\sqrt{2}k\nu_2\mu_L e^{\mathrm{i}(s\psi-\omega t)}\big\{\rho \mathrm{i}^{|s-2|+p}J_{jp}^{ss-2}[\sin] - \rho^*\mathrm{i}^{|s+2|+p}J_{jp}^{ss+2}[\sin]\\ & +\rho_2\mathrm{i}^{|s-1|+q}J_{jq}^{ss-1}[\cos] - \rho_2^*\mathrm{i}^{|s+1|+q}J_{jq}^{ss+1}[\cos]\big\}\end{aligned} \qquad (43)$$

for the u_A-wave. Here, $\alpha(1) = 1$ and $\alpha(s) = -1$ for $s \neq 1$.

The kinetic energy densities for these two waves are given by $w_K = w_0 w_M$ and $w_K = w_0 w_A$ with w_0 (20) and

$$w_M = \big(J_{jq}^{ss-1}[\cos]\big)^2 + \big(J_{jq}^{ss+1}[\cos]\big)^2 + 2\big(J_{jp}^{ss}[\sin]\big)^2 \qquad (44)$$

$$w_A = \big(J_{jp}^{ss-1}[1]\big)^2 + \big(J_{jp}^{ss+1}[1]\big)^2. \qquad (45)$$

The elastic energy densities and the energy flux density vector fields of the u_M- and u_A-waves are described by

$$\begin{aligned}\frac{w_E}{w_0} = {} & \frac{1}{4}\big(J_{jq}^{ss-2}[\sin\circ 2]\big)^2 + \frac{1}{4}\big(J_{jq}^{ss+2}[\sin\circ 2]\big)^2 + \frac{3}{2}\big(J_{jq}^{ss}[\sin\circ 2]\big)^2\\ & +\big(J_{jp}^{ss-1}[\cos\circ 2]\big)^2 + \big(J_{jp}^{ss+1}[\cos\circ 2]\big)^2\end{aligned} \qquad (46)$$

$$\begin{aligned}S'_A = {} & \beta(s)J_{jq}^{ss+1}[\cos]\big\{\alpha(s)J_{jq}^{ss-2}[\sin\circ 2] - J_{jq}^{ss}[\sin\circ 2]\big\}\\ & +\beta(-s)J_{jq}^{ss-1}[\cos]\big\{J_{jq}^{ss}[\sin\circ 2] - \alpha(-s)J_{jq}^{ss+2}[\sin\circ 2]\big\}\\ & +2J_{jp}^{ss}[\sin]\big\{\beta(-s)J_{jp}^{ss-1}[\cos\circ 2] - \beta(s)J_{jp}^{ss+1}[\cos\circ 2]\big\}\end{aligned} \qquad (47)$$

and

$$\frac{w_E}{w_0} = \big(J_{jp}^{ss-2}[\sin]\big)^2 + \big(J_{jp}^{ss+2}[\sin]\big)^2 + \big(J_{jq}^{ss-1}[\cos]\big)^2 + \big(J_{jq}^{ss+1}[\cos]\big)^2 \qquad (48)$$

$$S'_A/2 = \beta(1+s)J_{jp}^{ss+1}[1]J_{jp}^{ss+2}[\sin] - \beta(1-s)J_{jp}^{ss-1}[1]J_{jp}^{ss-2}[\sin] \qquad (49)$$

respectively.

For u_M- and u_A-storms ($s = 0$), the time-average energy flux vector $\boldsymbol{S}$ is identically zero at all points. The displacement vector $\boldsymbol{u}$ for u_M-storms has the azimuthal component vanishing everywhere and oscillating normal and radial components. The opposite situation occurs with u_A-storms. Figure 4 depicts the instantaneous displacement fields for the u_M- and the u_A-storms defined by the spherical harmonic Y_3^0. The normal u'_N- and the azimuthal u'_A-components have maximum intensity of oscillations in the same planes $z = \pm 0.7$, but at $R' = 0$ for the u_M-storm, and at $R' = 0.3$ for the u_A-storm.

Both u_M- and u_A-whirls have only azimuthal time-average energy fluxes ($\boldsymbol{S} = S_0 S'_A \boldsymbol{e}_A$, see figure 5), where S'_A depends only on R and z. Hence, they have circular energy flux lines. The spatial distributions of the azimuthal energy fluxes, described by $S' = S'(R, z)$, are quite different for the u_M- and the u_A-whirls, even though they are defined by the same spherical harmonic Y_4^2.

3.2. Tornadoes

When $s \neq 0$ and $\pi/2 < \theta_2 < \pi$, the field $\boldsymbol{W}_j^s$ (1) is composed from eigenwaves propagating in the solid angle Ω, satisfying the condition $2\pi < \Omega < 4\pi$. It is highly localized and has spiral energy flux lines similar to those of elastic tornadoes composed from longitudinal eigenwaves (see figure 5 in [5]). The step of these spirals tends to zero when θ_2 tends to π. The amplitude functions $\boldsymbol{W}$ (3) and $\boldsymbol{W}$ (4) specify two different polarization types ($u_{\rm M}$ and $u_{\rm A}$) of such elastic tornadoes formed from transverse waves. The properties of these fields are intermediate between those of the orthonormal beams (see section 2.1) and whirls (see section 3.1). For the fields defined by the zonal spherical harmonics ($s = 0$), energy flux lines lie in meridional planes.

4. Conclusion

Unique families of time-harmonic orthonormal beams and localized fields in an isotropic linear elastic medium, defined by the spherical harmonics Y_j^s, are presented. Each family consists of two sets of beams ($u_{\rm M}$- and $u_{\rm A}$-beams). They are obtained using expansions in transverse eigenwaves with the meridional and the azimuthal polarizations. Intensities and phases of these eigenwaves are specified by Y_j^s.

As in the case of fields formed from longitudinal plane waves, there are two different ways to compose families of orthonormal beams. The first results in two separate sets of orthonormal beams defined by the spherical harmonics Y_j^s with even and odd j, respectively. The second gives a complete system of orthonormal beams defined by the whole set of spherical harmonics Y_j^s. The presented localized fields include elastic storms, whirls and tornadoes. Since the elastic fields treated in this paper are formed from transverse plane waves, they bear some resemblance to electromagnetic orthonormal beams and localized fields discussed in [1–3].

References

[1] Borzdov G N 1999 *7th Int. Symp. on Recent Advances in Microwave Technology Proceedings* ed C Camacho Peñalosa and B S Rawat (Málaga: CEDMA) pp 169–72
Borzdov G N 2000 *Proc. Millennium Conf. on Antennas & Propagation, AP2000 (Davos, April 2000)* (Noordwijk: ESA) CD ROM SP-444: p0131.pdf, p0132.pdf
Borzdov G N 2000 *Proc. Bianisotropics 2000: 8th Int. Conf. on Electromagnetics of Complex Media (Lisbon, September 2000)* ed A M Barbosa and A L Topa (Lisbon: Instituto de Telecomucacões) pp 11–4, 55–8, 59–62
[2] Borzdov G N 2000 *Phys. Rev.* E **61** 4462
[3] Borzdov G N 2001 *Phys. Rev.* E **63** 036606
[4] Borzdov G N *J. Phys. A: Math. Gen.* **34** 6249–57 (preceding paper I)
[5] Borzdov G N *J. Phys. A: Math. Gen.* **34** 6259–67 (preceding paper II)
[6] Fedorov F I 1968 *Theory of Elastic Waves in Crystals* (New York: Plenum)
[7] Barkovsky L M, Borzdov G N and Fedorov F I 1983 *Zh. Prikl. Spektrosk.* **39** 996 (in Russian)
Barkovsky L M and Furs A N 1997 *J. Phys. A: Math. Gen.* **30** 4665
Furs A N and Barkovsky L M 1998 *J. Phys. A: Math. Gen.* **31** 3241